Pamukkale Üniversitesi Mühendislik Bilimleri Dergisi
Pamukkale University Journal of Engineering Sciences

Effect of Tungsten-Cobalt (Wco) nanoparticles on shear and flexural strength of adhesive joints

Tungsten-Kobalt (WCo) nanoparçacıklarının yapıştırma bağlantılarının kayma ve eğilme dayanımlarına etkisi

Mikail ASLAN[1], Mehmet Veysel ÇAKIR[2], Ahmed ALMOSSA[1]*

[1]Metallurgy and Materials Engineering, Gaziantep University, Gaziantep, Türkiye.
mikailsln@gmail.com, ahmedalmossa7@gmail.com.tr
[2]Mechanical Engineering, Kilis 7 Aralık University, Kilis, Türkiye.
cakir@kilis.edu.tr

Received/Geliş Tarihi: 13.12.2024 Revision/Düzeltme Tarihi: 19.01.2025 doi: 10.5505/pajes.2025.94572
Accepted/Kabul Tarihi: 25.01.2025 Research Article/Araştırma Makalesi

Abstract

The effects of Tungsten Cobalt (WCo) nanoparticle contribution on the shear and bending strengths are examined in adhesively bonded single-lap joints made with glass fiber-reinforced polymer (GFRP) substrates in this study. WCo particles were synthesized via mechanical alloying and added to epoxy adhesives at varying concentrations (1.0, 3.0, and 5.0 wt.%). The adhesive mixtures were used to bond GFRP plates in single-lap joints (SLJ), and their mechanical performance was evaluated under shear and bending loading conditions. The shear strength results indicate that the incorporation of 1.0 wt.% WCo increased shear strength by 68.5%, while 3.0 wt.% WCo yielded the highest improvement at 136%. However, the addition of 5.0% WCo led to a reduced enhancement (60%) due to nanoparticle agglomeration and local stress concentrations. Notably, the maximum bending stress was observed in the 3% WCo-containing specimens. Specifically, the bending load increased by 51.5%, from 61.96 MPa in the pure epoxy specimen to 93.85 MPa in the 3% WCo-reinforced specimen. Failure surface analysis revealed that WCo-reinforced samples exhibited light-fiber tear, thin-layer cohesive failures, and enhanced bonding properties due to increased viscosity and the filling of micro-voids. These findings suggest that WCo nanoparticles effectively improve the shear and bending performance of epoxy adhesives by enhancing interfacial bonding, ductility, and stress distribution mechanisms. The study provides insights into the potential of WCo-reinforced adhesives as a cost-effective and high-performance solution for engineering applications.

Keywords: WCo nanoparticles, Epoxy adhesive, Single-lap joints (SLJs), Shear strength, Flexural performance, Failure Modes

Öz

Bu çalışmada cam elyaf takviyeli polimer (GFRP) altlılarla yapılmış tek bindirmeli yapıştırma bağlantılarında Tungsten-Kobalt (WCo) parçacık katkısının kayma ve eğilme dayanımlarına etkileri incelenmektedir. WCo parçacıkları mekanik alaşım yöntemi ile sentezlenmiş ve epoksi yapıştırıcısına farklı konsantrasyonlarda (ağırlıkça % 1,0, 3,0 ve 5,0) eklenmiştir. Bu yapıştırıcı karışımları, GFRP plakalarını tek bindirmeli eklem (SLJ) şeklinde bağlamak için kullanılmış ve mekanik performansları kayma ve bükülme yükleri altında değerlendirilmiştir. Kayma dayanımı testleri, %1,0 WCo eklenmesinin kayma dayanımını %68,5 artırırken, %3,0 WCo katkısının %136 ile en yüksek iyileşmeyi sağladığını göstermiştir. Ancak %5,0 WCo eklenmesi, nanoparçacıkların topaklanması ve yerel gerilme yoğunlukları nedeniyle %60'lık daha az bir iyileşme ile sonuçlanmıştır. Dikkate değer bir şekilde, maksimum eğilme gerilmesi %3 WCo içeren numunelerde gözlemlendi. Özellikle, eğilme dayanımı %51,5 artarak, saf epoksi numunesinde 61,96 MPa iken %3 WCo takviyeli numunede 93,85 MPa'ya yükseldi. Hata yüzey analizi, WCo takviyeli örneklerde ince lif çekilmesi, ince tabaka kohezif arıza türleri ve mikro boşlukların dolması ile birlikte viskozite artışı nedeniyle geliştirilmiş bağlama özellikleri sergilediğini ortaya koymuştur. Bu bulgular, WCo nanoparçacıklarının arayüzey bağlanmasını, sünekliği ve gerilme dağılım mekanizmalarını iyileştirerek epoksi yapıştırıcılarının kayma ve eğilme performansını etkili bir şekilde artırdığını göstermektedir. Çalışma, WCo takviyeli yapıştırıcıların, mühendislik uygulamaları için maliyet açısından etkin ve yüksek performanslı bir çözüm olma potansiyeline sahip olduğunu vurgulamaktaydı.

Anahtar kelimeler: WCo nanoparçacıkları, Epoksi yapıştırıcı, Tek katmanlı eklemler (SLJ'ler), Kayma dayanımı, Eğilme performansı, Hata modları

1 Introduction

With rapid technological advancements and increasing industrial competition, the demand for lightweight materials with high durability and performance has significantly increased. To meet this demand, The adoption of combined materials has grown more common across various sectors, including defense and commercial air travel, robotic limbs, and the automobile sector [1]. Specifically, for use in the aviation and defense industries, composite materials, which are lighter and more durable than metals, are continuously being designed and produced. In the aerospace industry, where weight and strength factors are of critical importance, the use of composite materials in airplane fuselages has become inevitable [2].

Due to limitations such as material size, ease of manufacturing, or transportation, it is often not possible to manufacture a structure without joints. Various techniques are used to join two different materials, including welding, riveting, and adhesive bonding. Adhesive bonding, in particular, has been a widely used method for many years in the aerospace and automotive sectors because it offers several advantages over traditional mechanical fastening systems [3]. Scientists created adhesive bonding methods to overcome the drawbacks of traditional mechanical fastening. This approach is especially

*Corresponding author/Yazışılan Yazar

useful for connecting fiber-reinforced polymer composites, as it reduces typical problems linked to mechanical fasteners, such as stress buildup, increased mass, and layer separation [4]. The adhesive bonding technique offers numerous benefits and plays a significant role in the industry. It simplifies assembly by reducing the number of parts and provides flexibility in the design process. Additionally, it provides engineering benefits, including an excellent strength-to-weight ratio, enhanced resistance to fatigue, minimal stress concentration, and better vibration damping characteristics [5, 6]. Thanks to these attributes, adhesive bonding is widely used in important sectors of the industry and continues to be the preferred method. Adhesive-bonded connections are now commonly employed in numerous applications, including the automotive [7], textile [8], aerospace [9], and medical device [10] industries, as well as in the repair of composite structures [11].

SLJs are the types of connection that is frequently current especially in engineering fields [12-15]. They are practical, affordable, and simple to produce. The uncomplicated and effective design of SLJs enables consistent assessment of the mechanical features of adhesively bonded joints (ABJ) [16]. Extensive research on bonded SLJs has been carried out through both experimental [17-19] and numerical methods [19-21]. Regardless of the bonding method, the natural drawbacks of an epoxy matrix, including its brittleness and low toughness, adversely affect the bonding strength of the composite component. [22, 23]. To enhance the strength of composite joints, researchers have incorporated various nanofillers, including CNTs [24], graphene [25], graphene oxide, polyurethane nanofibers [26], nylon nanofiber [27], [28], silica [29], and nano iron oxide [30], into the epoxy matrix. Saraç et al. [31] investigated the impact of the contribution of nano-Al_2o_3 and nano-Ti_2O_3 on the strength of the joints bound by epoxy adhesive. Nano-Al_2O_3 particles were found to be the most effective in enhancing the failure resistance of the ABJs. The largest strength progression, which reached an increase of 97 %, was obtained in samples with 20 mm overlap length, 4 % nano-Al_2O_3 by weight. A study by Çakır et al. [25] investigated the impact of different graphene nanoplatelets (GNPs) concentrations in the epoxy-based adhesive on the shear and bending features of GFRP-GFRP joints. GNPs were added to the epoxy at concentrations of 0.1, 0.2, 0.3, 0.4, and 0.5 wt. %, with GFRP serving as the adherent material. Failure modes were assessed by capturing images of both the front and rear sides of the samples post-testing. The findings indicated that adding GNP notably enhanced the chemical accordance between the adhesive layer and the GFRP adherend surfaces, enhanced surface wetting, and ultimately increased the joint shear strength. Additionally, the inclusion of GNP in the epoxy promotes greater flexibility, leading to a more even stress distribution across the joint and, ultimately, improved strength. In the study [31], Shear strength and thermal features of ABJs were studied using nanoparticle-enhanced adhesives in carbon fiber-reinforced composite materials (CFRP). The epoxy resin employed was diglycidyl ether bisphenol A (DGEBA). SLJ tests were performed in ABJs reinforced with 1 % multi-walled carbon nanotubes (MWCNT), and 3 % to 7 % with silicon dioxide (SiO_2) particles. The shear strengths of these modified adhesives were compared to those of pure epoxy resin. The results presented that the mixture of 1% MWCNT and 3% SiO_2 provided the most significant improvement, with a 46% increase in shear strength. Combinations of 1% MWCNT with 5% SiO_2, 1% MWCNT, and 1% MWCNT with 7% SiO_2 resulted in increment of 32%, 14%, and 5%, respectively. The tensile test results indicated that the tensile strength of pure epoxy was 5953 N, whereas that of the composite with 1% MWCNT and 3% SiO_2 was 8738 N, reflecting an improvement of approximately 47%.

As mentioned above, various micro- or nanoparticles have been used to enhance the performance of adhesives. Each nanoparticle displays distinct physical properties that are not possible at the macro scale. Metallic nanoparticles are used in a wide range of engineering applications.

Metallic nanoparticles can be synthesized from any element in the periodic table, with common types including nanogold, nanosilver, and metal oxides like alumina (Al_2O_3) and zirconium (ZrO_2). They grow polymers' mechanical, electrical, optical, and magnetic features [33]. However, a review of the literature indicates that research into the use of tungsten or tungsten alloy particles as reinforcements in adhesives is almost nonexistent except for the study [32] . The production of tungsten alloys can be done with methods of powder metallurgy [33], laser directed energy deposition [34], ball milling [35] and single-laser bed fusion [36]. In the study [37], The W-Ni-Co tungsten alloys, fabricated through mechanical alloying, have been investigated. The resulting microstructure consists of a fine, uniformly distributed γ(Ni,Co) binder phase, along with a high volume of twinned structures, which contributes to the enhancement of the mechanical properties

In this paper, the WCo alloys were synthesized via mechanical alloying. SLJs in industrial settings are subjected to various types of loads, including tension, shear, bending, and impact, or combinations of these forces. As a result, the effective design of these joints requires a thorough understanding of stress, crack mechanisms, and damage types under different loading scenarios. This study explored the impact of incorporating tungsten alloy particles into a marketable epoxy-based adhesive on the shear and flexural strength of SLJs bonded with GFRP plates. Additionally, failure modes of SLJs under numerous circumstances were analyzed. The primary objective is to develop a cost-effective, high-performance adhesive suitable for broad engineering applications.

2 Experimental Parts

2.1 Materials

Tungsten (density: 19.3 g/cm^3, resistivity: 5.6 microhm-cm, melting temperature: 3387 °C and cubic size) and cobalt (density: 8.92 g/cm^3, resistivity: 6.24 microhm-cm, melting temperature: 1495 °C and hexagonal size) powders with 99.9% purity were obtained from Nanografi Nano Technology, with an average particle size of 45 µm. GFRP composites (G10-FR4, 2 mm thick, density: 1.82, tensile strength: 363 MPa, elastic modules: 18.65 GPa, flexural strength: 413 MPa and flexural modules: 18.65 GPa) were sourced from Küçükparmak Mühendislik in Turkey, and laminating resin components A and B were supplied by ADS Chemistry.

Preparation of W-Co alloys

Elemental powder precursors, including W (85% wt) and Co (15% wt), were used as the starting materials for the process. The mechanical alloying (MA) was carried out using a Retsch PM 100 planetary high-energy ball mill, equipped with 120 mL stainless steel grinding jars. The mill operated for 50 hours with 10 mm diameter stainless steel balls, maintaining a ball-to-powder weight ratio of 15:1, a rotation speed of 300 rpm, and

direction reversals every 10 minutes. The mill was run for 10 minutes and turned off for 10 minutes to prevent the temperature from increasing excessively. The SEM images of the produced WCo alloy is illustrated in Figure 1.

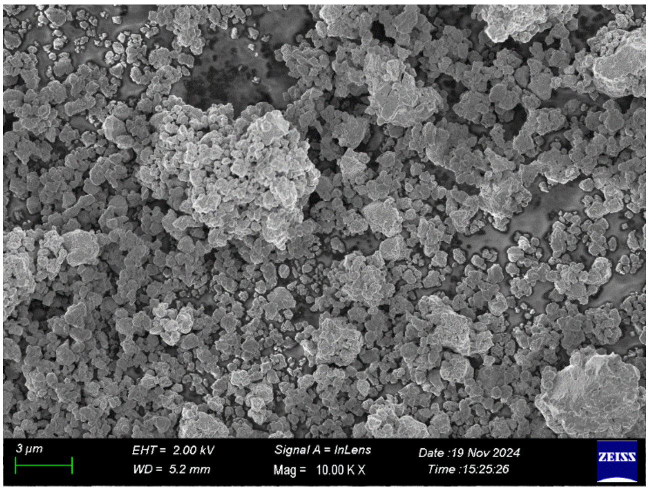

Figure 1 The SEM images of the produced WCo alloy

2.3 Preparation of adhesively bonded single lap joints

The tungsten alloy particles were incorporated into the epoxy resin (10 g) at concentrations of 1, 3, and 5 wt.%, and the mixture was weighed accordingly. The powder compounds and resin were placed in a beaker and mixed for 30 minutes using a magnetic stirrer. Afterward, the hardener was added in a resin-to-hardener ratio of 2:1 by weight. The resulting mixture was stirred for 3 hours at 600 rpm. To ensure uniformity, the compound was manually mixed for an additional 5 minutes and then left to dry at room temperature.

Plates measuring 100 mm by 25 mm were cut using a guillotine from GFRP sheets to serve as substrates. To improve bonds between the adhesive and the adherends, the bonding surfaces were roughened with 300-grit silicon carbide sandpaper, following ASTM D5868–01 standards. The adherend surfaces were then cleaned with acetone to eliminate any contaminants.

The SLJ configurations of the specimens are shown in Figure 2. An aluminum mold (Figure 3) was used to connect the 100×25×2 mm plates with an overlap of 25 mm. This mold also kept the bond thickness constant at 0.3 mm. For direct shear strength testing, end tabs (25×25 mm) were added to the specimens.

The mold was specifically designed to create a uniform adhesive layer thickness of 0.3 mm. Five samples were prepared for each configuration using this mold. After bonding, the samples were held for 24 hours in the mold for curing. Following this, they were removed from the mold and allowed to be cured outside for five days to ensure complete curing. Afterward, the samples were exposed to single-lap shear tests.

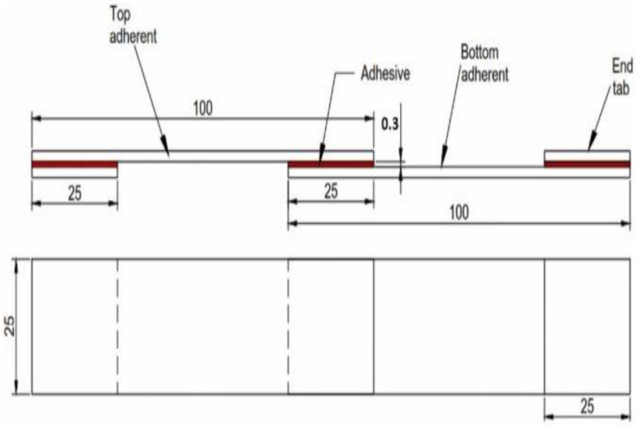

Figure 2 Dimensions of single lap joint configuration

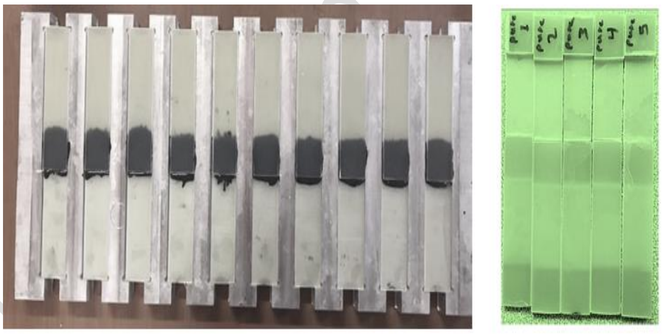

Figure 3 Specifically designed mold

3 Results and Discussion

3.1 Lap Shear Test

Typically, single-lap shear tests are performed to assess the shear performance of adhesively bonded SLJs in the industry. [24]. This study investigated how the addition of WCo alloy affects the shear performance of these ABJs, utilizing the Shimadzu AG-X testing machine (see Figure 4).

According to ASTM D5868-01 standards, tensile loads were applied to the specimens at a crosshead speed of 1 mm/min. GFRP end tabs, measuring 25 mm × 25 mm, were used to apply pure shear loads on the specimens and to secure them in the grips. Load-displacement data were recorded using a data acquisition system connected to the tensile testing machine. The maximum shear strength of each specimen was calculated using the following formula.

$$\tau_{max} = \frac{F}{\ell \times b} \quad (1)$$

Here, F denotes the maximum load, while l and b refer to the bonded lap length (25 mm) and the depth (0.3 mm) of the adhesive connection area, respectively. To ensure reliability, a minimum of five specimens from each configuration were tested.

Table 1 Single lap shear test results

Sample Code	Epoxy adhesive (wt.%)	WCo (wt.%)	Maximum Load (N)	Maximum Shear Stress (MPa)	Enhancement (%)
Pure	100.0	0.0	3020.9±234	4.83±0.38	0.0
WCo-1%	99.0	1.0	5091.2±254	8.15±0.41	68.5
WCo-3%	97.0	3.0	7134.2±263	11.41±0.42	136.1
WCo-5%	95.0	5.0	4838.5±389	7.74±0.62	60.1

Figure 4. Performing of lap shear tests on tensile test machine

The lap shear test results are presented in Table 1. Compared to the unmodified specimens, the shear strength of the 1.0 wt% WCo-modified specimens increased by 68.5%. The highest shear strength improvement was observed in the 3.0 wt% WCo specimens, reaching 136%. However, in the 5.0 wt% WCo specimens, this improvement decreased to 60%. This reduction is attributed to the limitations associated with adding nanoparticles to epoxy-based adhesives. When these limits are exceeded, nanoparticle agglomeration can occur, leading to local stress concentrations and a subsequent reduction in joint strength [38].Tensile load-extension curve analysis of both pure epoxy adhesive and WCo-modified SLJ specimens revealed that the maximum elongation at failure (1.766 mm) was observed in the 3.0 wt% WCo specimens. In contrast, the unmodified specimens exhibited a failure elongation of 0.72 mm, representing a 145% improvement. Overall, these findings suggest that the incorporation of WCo significantly enhances the ductility and toughness of the adhesive (Figure 5).

3.2 Three-point bending test

The effect of incorporating tungsten carbide (WCo) into the adhesive on the flexural strength of bonded SLJs was investigated using three-point bending tests (see Figure 5). The test setup and specimen dimensions are illustrated in Figure 5. The distance between the two supports (the span length), was about 16 times the sample thickness in accordance with the ASTM D790-17. and the bending load was applied at a rate of 2 mm/min. To ensure proper horizontal alignment of the specimens during the test, a 25 × 25 mm glass fiber reinforced plastic (GFRP) protrusion was added to one of the support points.

During the bending test, the applied load causes compressive stress between the adhesive and upper plate, while the lower plate and adhesive cause tensile stress (Figure 5). The load applied to the midpoint of SLJ generates a compound loading impact categorized by a fixed transverse cutting force and growing bending moment along the adhesive overlap area. The maximum flexible stress is figure out by the following equation:

$$\sigma_f = \frac{3PL}{2wd^2} \quad (2)$$

Where: σ_f = bending stress at midpoint (MPa), P = load (N), L = support span (mm), b = width of joint (mm), and d = depth of joint (mm).

The bending load–displacement curves obtained from the three-point bending tests are presented in Figure 6. As shown in the figure, two peak points are observed in all specimens except for the 3% WCo reinforced sample. The load increases linearly until the first peak until the first peak due to higher peeling stress at the free edge of the substrate sustained to stress. The first peak corresponds to the maximum load-bearing point. Once this maximum load is reached, the SLJs begin to separate from the free edge, leading to a decrease in load and the initiation of crack propagation. The load then increases again until the second peak, which indicates either failure of the GFRP layer or complete separation of the SLJs. After the first peak, the subsequent load–displacement behavior is influenced by factors such as substrate stiffness, substrate thickness, and other material properties. Therefore, the load at the first peak is the primary value considered in bending stress calculations. In the 3% WCo-reinforced samples, sudden fracture occurs after reaching the maximum load, indicating that excessive loading causes the complete separation of the SLJs. In other configurations, SLJ separation occurs relatively quickly. All WCo-containing specimens demonstrated superior load-bearing capacity compared to the unreinforced epoxy specimens, as illustrated in Figure 7. Notably, the maximum bending stress was observed in the 3% WCo-containing specimen (Figure 7). While the bending load for the pure epoxy specimen was 61.96 MPa, it increased by approximately 51.5% in the 3% WCo-containing specimen, reaching 93.85 MPa. Conversely, as seen in the single shear test, the 5% WCo-containing specimens exhibited a reduction in both shear strength and bending strength. This decline is likely due to agglomeration and related material disruptions, which impair load transfer between the nanoparticles and the adhesive.

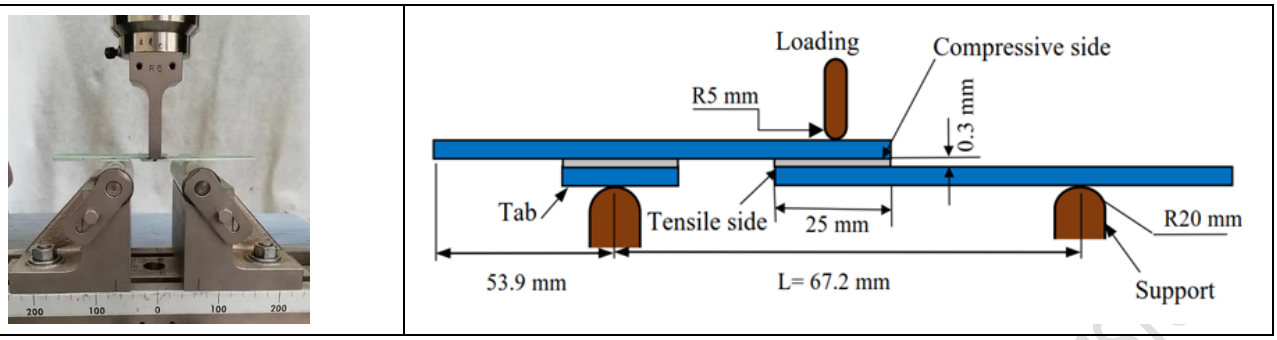

Figure 5. Performing of three-point bending test and sample dimensions.

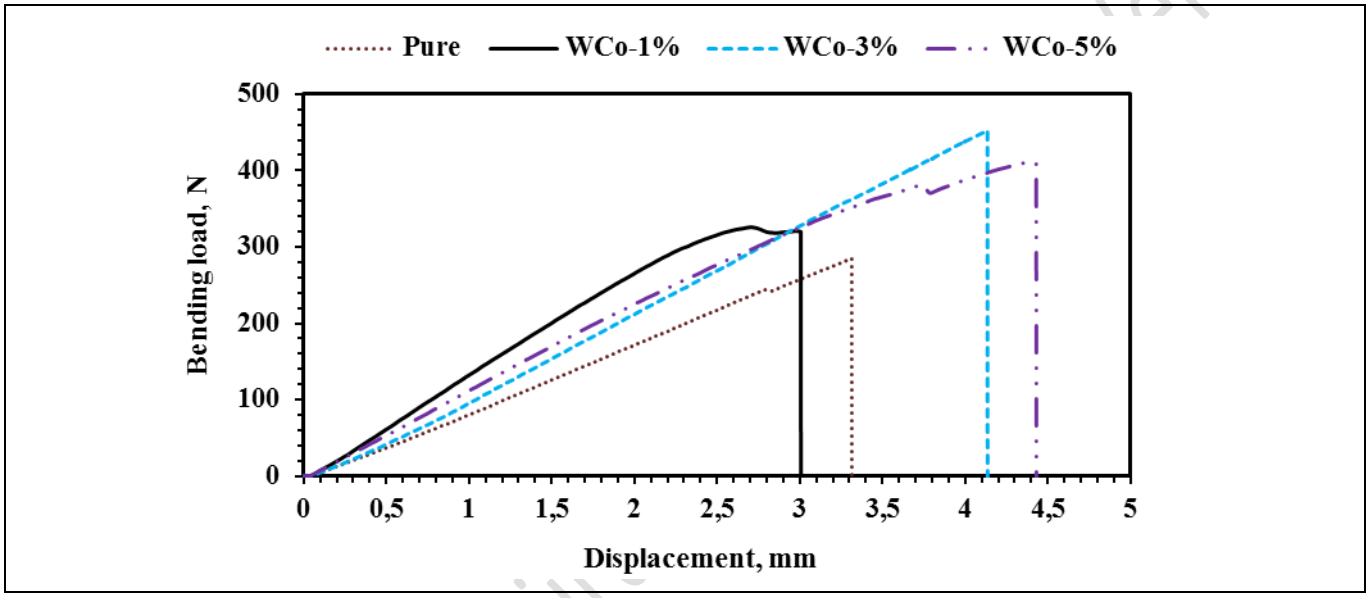

Figure 6 Bending load-displacement curves of specimens after three-point bending tests.

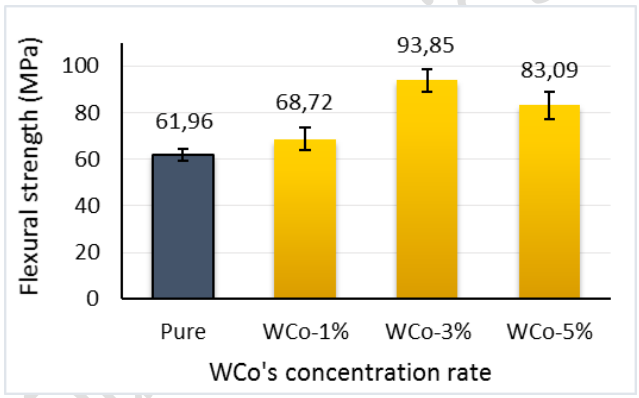

Figure 7. Flexural Strengths as a Function of Tungsten Alloy

3.3 Failure Analysis

To gain a comprehensive understanding of the mechanical properties of pure and WCo-reinforced adhesives under single shear loading, it is essential to analyze the failure modes. The failure mode serves as an indicator of both the quality of the adhesive joints and the bond's overall strength. Following the shear test, the surfaces of the pure epoxy adhesive samples exhibited adhesive-type failure, with the surfaces remaining smooth (Figure 8). Adhesive failure is characterized by interfacial separation, where the bonded component completely detaches from one side. This indicates that the adhesive joint has detached from the bonding surface, with no adhesive residue remaining at the interface.

The macro-images of the WCo-reinforced samples reveal a rough surface morphology. In the 1.0% and 3.0% WCo-reinforced samples, fine cohesive failure and fine fiber pullout damages are evident. Notably, in some overlap regions, a thin adhesive layer has dispersed, a phenomenon referred to as thin-layer cohesion failure. This type of failure, characterized by the adhesive layer itself breaking, indicates that high shear stresses were experienced during loading. Fiber pullout suggests that the connection itself did not fail, but the damage is confined to the bonded material [39]. In the 3.0% WCo-reinforced samples, fiber damage is significantly more pronounced. The damage surfaces of the 5.0% WCo-reinforced samples are markedly rougher due to the higher reinforcement ratio, although adhesive-type failure was observed. The pure epoxy adhesive was highly fluid, leading to seepage from the bonding region and the formation of voids in certain areas. However, the addition of WCo increased the adhesive's viscosity, thereby preventing seepage and the formation of voids. This indicates that WCo particles enhance bond strength by filling micro-voids on the substrate surface and creating new contact points [40].

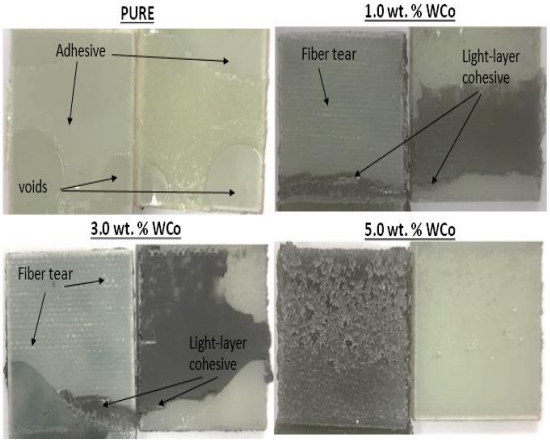

Figure 8. Failure surfaces of test samples after single lap-shear tests

The strength of adhesive joints is highly sensitive to the direction of applied stress. While abrasive bonding joints (ABJs) exhibit strong resistance to tensile and shear stresses, bending loads create both tensile and shear stresses, resulting in localized stress concentrations over a small area. In adhesive joints, one free end experiences tensile stress, while the other is exposed to compressive stress. These opposing forces produce tensile peeling stress in the positive direction and compressive peeling stress in the negative direction. Consequently, cracks initiate at the connection point subjected to positive peeling stress (crack initiation) and propagate across the entire bonded area, ultimately leading to joint failure [41]. Upon examining the fracture surfaces of adhesive joints subjected to three-point bending loading (Figure 9), it was found that pure epoxy adhesive joints failed exclusively through an adhesive failure mode. This failure type corresponds to the lowest bending strength observed during the bending test. When 1.0% WCo was added, thin-layer cohesive failure was observed. In the 3.0% WCo-reinforced sample, damage included both thin-layer cohesive failure and fine fiber pullout. This type of failure is comparable to the failure behavior observed under shear loading conditions (Figure 8). The light-fiber tear and thin-layer cohesive failures, accompanied by instances of fiber breakage, indicate that WCo reinforcement enhances both shear and bending performance. These failure mechanisms suggest effective adhesion between the adhesive layer and the substrates, highlighting a strong and well-developed bonding interface.

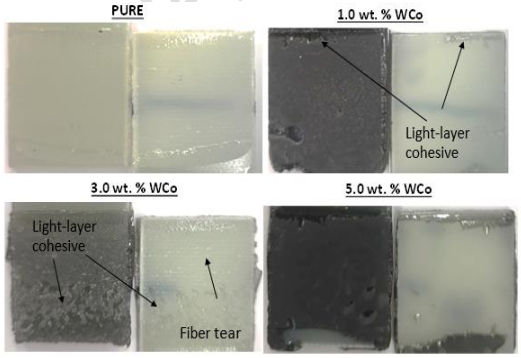

Figure 9. Failure surfaces of test samples after three-point bending tests

The effective use of adhesive joints will play a crucial role in assessing their strength under various external loads in the future. The addition of WCo particles enhanced the strength of the adhesively bonded single-lap joints when subjected to shear and flexural loads. Notably, the sliding and bending strengths of adhesive connections modified with 3.0% WCo showed the most significant improvements compared to those using pure adhesive. WCO particles positively influence load transfer between substrates and adhesives by introducing new mechanical ways. This improvement leads to stronger adhesion forces. The use of WCo additives alters joint failure modes, avoiding light-layer cohesive and fiber-tear modes, which in turn increases the vineyard forces. This observation aligns with findings from mechanical experiments. High WCo content (5%) has led to a decrease in connection strength due to stress concentration points and nanoparticle agglomeration that could lead to local failure. This indicates that the contribution rate of WCO particles needs to be properly regulated.

4 Conclusion

This study investigated the effects of incorporating tungsten-cobalt (WCo) alloy nanoparticles into epoxy adhesive systems on the mechanical performance of single-lap joints (SLJs) bonded to glass fiber-reinforced polymer (GFRP) substrates.

The experimental results from shear testing demonstrated a significant improvement in the shear strength of SLJs as the WCo content increased, with the 3.0 wt% WCo-modified adhesive achieving the highest shear strength enhancement of 136% compared to the unmodified epoxy adhesive. However, at the highest WCo content of 5.0 wt%, a reduction in shear strength was observed, likely due to nanoparticle agglomeration, which can lead to stress concentration points and local failure. Additionally, three-point bending tests revealed that WCo incorporation significantly improved the ductility and flexural strength of the adhesive joints. The results showed that the elongation at failure increased by 145% in the 3.0 wt% WCo specimens compared to the unmodified epoxy.

Failure analysis of the shear and bending specimens provided further insights into the mechanisms behind the observed performance improvements. Pure epoxy adhesive specimens exhibited adhesive-type failure modes with smooth fracture surfaces, indicative of interfacial failure under tensile loading. However, WCo-modified specimens displayed fine cohesive failure, thin-layer cohesive failures, and light-fiber tear damages. These failure mechanisms suggest that WCo particles improve adhesion by creating better stress distribution, reducing localized stress concentrations, and enhancing interfacial compatibility with the substrate. Moreover, the rough surface morphology observed in the failure regions of WCo-modified SLJs points to effective load transfer facilitated by the nanoparticles, which further strengthens the joint under loading conditions. Thus, the originality of this study lies in examining the reinforcement effects of tungsten alloys in glass fiber reinforced polymer. This represents a significant advancement and innovation in the polymer composites sector.

5 Author contribution statements

Author 1 contributed to the conceptualization, supervision, experimental design, data collection, and writing of the original draft. Author 2 participated in conceptualization, experimental design, and writing the original draft. Author 3 was involved in experimental design, data collection, and writing the original draft.

6 Conflicts of interest

The authors confirm that they have no financial interests or personal affiliations that might have affected the research presented in this paper.

7 References

[1] Torralba JD, Da Costa CE, and Velasco F. P/M aluminum matrix composites: an overview. Journal of Materials Processing Technology 2003; 133: 203-206.

[2] Lin Y, Gigliotti M, Lafarie-Frenot MC, Bai J, Marchand D, and Mellier D. Experimental study to assess the effect of carbon nanotube addition on the through-thickness electrical conductivity of CFRP laminates for aircraft applications. Composites Part B: Engineering 2015; 76: 31-37.

[3] Kadioglu F. Mechanical behaviour of adhesively single lap joint under buckling conditions. Chinese Journal of Aeronautics 2021; 34: 154-164.

[4] Dhilipkumar T and Rajesh M. Effect of using multiwall carbon nanotube reinforced epoxy adhesive in enhancing glass fiber reinforced polymer composite through cocure manufacturing technique. Polymer Composites 2021; 42: 3758-3772.

[5] Qin M and Dzenis YA. Analysis of single lap adhesive composite joints with delaminated adherends. Composites Part B: Engineering 2003; 34: 167-173.

[6] Park H and Kim H. Damage resistance of single lap adhesive composite joints by transverse ice impact. International Journal of Impact Engineering 2010; 37: 177-184.

[7] Cavezza F, Boehm M, Terryn H, and Hauffman TJM. A review on adhesively bonded aluminium joints in the automotive industry. 2020; 10: 730.

[8] Petrie EM. Adhesive bonding of textiles: principles, types of adhesive and methods of use. Joining textiles 2013; 21: 225-274.

[9] Hart-Smith J, "Aerospace industry applications of adhesive bonding," in *Adhesive bonding*: Elsevier, 2021, 763-800.

[10] Tavakoli SM, Pullen DA, and Dunkerton SB. A review of adhesive bonding techniques for joining medical materials. Assembly Automation 2005; 25: 100-105.

[11] Karaoğlan H, Erkliğ A, Doğan NF, and Bulut M. A comparative study on adhesive properties of nanoparticle reinforced epoxy bonded single-strap repaired composites. International Polymer Processing 2024; 39: 70-79.

[12] Shu Y, Qiang X, Jiang X, Xiao Y, and Dong H. Long-term performance of single-lap joints: Review, challenges and prospects in civil engineering. Engineering Reports 2023; 6: e12769.

[13] Turaga UVRS and Sun CT. Improved design for metallic and composite single-lap joints. Journal of Aircraft 2008; 45: 440-447.

[14] De Sousa C, Campilho R, Marques EAS, Costa M, and da Silva LFM. Overview of different strength prediction techniques for single-lap bonded joints. Proceedings of the Institution of Mechanical Engineers, Part L: Journal of Materials: Design and Applications 2017; 231: 210-223.

[15] Dominguez F and Carral L. A review of formulations to design an adhesive single-lap joint for use in marine applications. Brodogradnja: An International Journal of Naval Architecture and Ocean Engineering for Research and Development 2020; 71: 89-119.

[16] Sülü İY. Mechanical behavior of single-lap and double-lap adhesive joined composite parts. Materials Testing 2017; 59: 1019-1026.

[17] Shu Y, Qiang X, Jiang X, and Li Y. Experimental and theoretical study on mechanical performance of Fe-SMA/steel single lap joints. Thin-Walled Structures 2024; 199: 111824.

[18] Zhao L-C, Karimi S, and Xu L. An experimental investigation of static and fatigue behavior of various adhesive single lap joints under bending loads subjected to hygrothermal and thermal conditions. The Journal of Adhesion 2024; 100: 845-866.

[19] Akkasali NK and Biswas S. Influence of reinforcement on vibration control in adhesively bonded single lap joints: a numerical and experimental validation. Engineering Research Express 2024; 6: 035558.

[20] Metehri A, Madani K, and Campilho RDSG. Numerical analysis of the geometrical modifications effects on the tensile strength of bonded single-lap joints. International Journal of Adhesion and Adhesives 2024; 134: 103814.

[21] Xiang S, Cheng B, Wang J, Li D, and Yan X. Behavior of hybrid bonded/bolted GFRP single-lap joint under static tensile loading: An experimental and numerical study. Journal of Composite Materials 2024; 0: 219.

[22] Budhe S, Banea MD, de Barros S, and Da Silva LFM. An updated review of adhesively bonded joints in composite materials. International journal of adhesion and adhesives 2017; 72: 30-42.

[23] Kumar A, Kumar K, Ghosh PK, Rathi A, and Yadav KL. MWCNTs toward superior strength of epoxy adhesive joint on mild steel adherent. Composites Part B: Engineering 2018; 143: 207-216.

[24] Özbek Ö and Çakır MV. MWCNT and nano-silica hybrids effect on mechanical and fracture characterization of single lap joints of GFRP plates. International Journal of Adhesion and Adhesives 2022; 117: 103159.

[25] Çakır MV, Erkliğ A, and Ahmed BF. Graphene nanoparticle effect on flexural and shear behaviors of adhesively bonded single lap joints of GFRP composites. Journal of the Brazilian Society of Mechanical Sciences and Engineering 2021; 43: 1-11.

[26] Öteyaka MÖ, Aybar K, and Öteyaka HC. A comparative study of the effect of polyurethane nanofiber and powders filler on the mechanical properties of carbon fiber and glass fiber composites. Pamukkale Üniversitesi Mühendislik Bilimleri Dergisi 2022; 28: 51-57.

[27] Yilmaz M, Ekrem M, and Avci A. Impact resistance of composite to aluminum single lap joints reinforced with graphene doped nylon 6.6 nanofibers. International Journal of Adhesion and Adhesives 2024; 128: 103565.

[28] Demir TN, Yuksel Yilmaz AN, and Celik Bedeloglu A. Investigation of mechanical properties of aluminum–glass fiber-reinforced polyester composite joints bonded with structural epoxy adhesives reinforced with silicon dioxide and graphene oxide particles. International Journal of Adhesion and Adhesives 2023; 126: 103481.

[29] Razavi N, Ayatollahi MR, Giv AN, and Khoramishad H. Single lap joints bonded with structural adhesives reinforced with a mixture of silica nanoparticles and multi walled carbon nanotubes. International Journal of Adhesion and Adhesives 2018; 80: 76-86.

[30] Vattathurvalappil SH and Haq M. Thermomechanical characterization of Nano-Fe3O4 reinforced thermoplastic adhesives and single lap-joints. Composites Part B: Engineering 2019; 175: 107162.
[31] Ekrem M, Koyunbakan M, and Ünal B. Investigation of the mechanical and thermal properties of epoxy adhesives reinforced by carbon nanotubes and silicon dioxide nanoparticles in single-lap joints. Journal of Adhesion Science and Technology 2024; 38: 1-16.
[32] Aslan M, Yaykaşlı H, and Eskalen H. The W-Zn-Co-Y2O3 alloys synthesized by a secondary ball milling method and their effects on adhesion performance of single lap joints of aluminum composites. Materials Today Communications 2023; 36: 106723.
[33] Candela S *et al.* Effects of micro-sized TiC on the cracking behavior of additively manufactured tungsten. Materials Letters 2025; 137969.
[34] Hao Z *et al.* Microstructure evolution and mechanical properties of tungsten alloy prepared by laser directed energy deposition. Journal of Alloys and Compounds 2025; 1010: 177056.
[35] Yang R *et al.* Microstructure and mechanical properties of ultrafine-grained W-Ni-Al alloys prepared via in-situ precipitation. Journal of Alloys and Compounds 2025; 1010: 178002.
[36] Dai D, Wang L, Chen T, Shi K, and Zhang H. Dual-laser powder bed fusion of difficult-to-process tungsten heavy-alloy: Inhibition of inferior defects and integrated fabrication of thin-walled overhanging structures. Thin-Walled Structures 2025; 208: 112827.
[37] Chen C-L and Ma S-H. Study on characteristics and sintering behavior of W-Ni-Co tungsten heavy alloy by a secondary ball milling method. Journal of Alloys and Compounds 2018; 731: 78-83.
[38] Cakir MV and Kinay D. MWCNT, nano-silica, and nano-clay additives effects on adhesion performance of dissimilar materials bonded joints. Polymer Composites 2021; 42: 5880-5892.
[39] Peng H, Zhou T, Shangguan L, and Cheng R. Effect of Temperature and Humidity Coupling on the Ageing Failure of Carbon Fiber Composite/Titanium Bonded Joints. Polymers 2024; 16: 952.
[40] Banea MD, Rosioara M, Carbas RJC, and Da Silva LFM. Multi-material adhesive joints for automotive industry. Composites Part B: Engineering 2018; 151: 71-77.
[41] Özbek Ö and Çakır MV. MWCNT and nano-silica hybrids effect on mechanical and fracture characterization of single lap joints of GFRP plates. International Journal of Adhesion and Adhesives 2022; 117: 103159.